Earthquakes and Structures, *Vol. 26, No. 1 (2024) 49-58*
https://doi.org/10.12989/eas.2024.26.1.049

Experimental study on replaceable precast concrete beam-column connections

Seung-Ho Choi[1], Sang-Hoon Lee[2], Jae-Hyun Kim[3], Inwook Heo[3], Hoseong Jeong[3] and Kang Su Kim*[2]

[1]*Department of Disaster Management and Fire Safety Engineering, University of Seoul, 163 Siripdae-ro, Dongdaemun-gu, Seoul 02504, Korea*
[2]*Department of Architectural Engineering and the Smart City Interdisciplinary Major Program, University of Seoul, 163 Siripdae-ro, Dongdaemun-gu, Seoul 02504, Korea*
[3]*Department of Architectural Engineering, University of Seoul, 163 Siripdae-ro, Dongdaemun-gu, Seoul 02504, Korea*

(Received March 15, 2023, Revised June 22, 2023, Accepted December 19, 2023)

Abstract. The purpose of this study was to develop a system capable of restoring the seismic performance of a precast concrete (PC) connection damaged by an earthquake. The developed PC connection consists of a top-and-seat angle, post-tensioning (PT) tendons, and U-shaped steel. The PC beam can be replaced by cutting the PT tendons in the event of damage. In addition, the seismic performance of the developed PC beam-column connection was evaluated experimentally. A PC beam-column connection specimen was fabricated, and a quasistatic cyclic loading test was conducted to a maximum drift ratio of 2.3%. Subsequently, the PC beam was replaced by a new PC beam, and the repaired PC connection was loaded to a maximum drift ratio of 5.1%. The structural performance of the repaired PC connection was then compared with that of the original PC connection. The difference in the load at the drift ratio of 2.3% between the original and the repaired PC specimens was only 0.2%. The residual drift ratio in the repaired PC specimen did not exceed 1.0% at the 2.0 % drift ratio cycles, which satisfies the life safety performance level specified in ACI 374.2R-13. When the developed PC connection system is used, structural performance can be restored by rapidly replacing the damaged elements.

Keywords: beam-column joint; precast concrete; replaceable; seismic performance

1. Introduction

In building design, various types of lateral-load-resisting systems are used to meet seismic performance requirements. Among them, reinforced concrete (RC) moment-resisting frames or dual frame systems are frequently used because of superior integrity of their beam-column connections as well as their cost-effectiveness (Parastesh *et al.* 2014). Therefore, many studies have been conducted on the RC beam-column connections (Paulay *et al.* 1978, Barbhuiya and Choudhury 2015, Tazarv *et al.* 2020, Zhang and Li 2020, Peloso *et al.* 2020, Pauletta *et al.* 2021, Choi *et al.* 2022a, Frappa and Pauletta 2022, Arash Karimi 2022). Precast concrete (PC) systems are frequently applied to control the quality of members and shorten the duration of a construction project. In general, PC members are individually manufactured in a factory and assembled on site with a small amount of concrete casting or grouting work (Yu *et al.* 2019, Choi *et al.* 2022b). However, because structural integrity may be lacking in the PC system, studies to improve integrity performance have been conducted (Li *et al.* 2009, Jin *et al.* 2016, Lu *et al.* 2018, Hwang *et al.* 2021, Kim *et al.* 2021, Choi *et al.* 2021, Choi *et al.* 2022c, Han *et al.* 2022). Li *et al.* (2009) developed a precast hybrid-steel concrete connection. Han *et al.* (2022) conducted an experimental study of steel-concrete composite beams with prestressed wide flange and hollowed steel web. Lu *et al.* (2018) have proposed a new type of connection to improve the joint integrity by using U-shaped bars.

Even in earthquake-resistant structures, local damage and lateral deformation of the beam-column connection inevitably occur in the event of an earthquake. Damage to the beam-column connection can require major retrofitting and reconstruction works, which impose a significant financial and social burden on owners and users. In addition, the secondary damage caused by the inability to use the structure during the earthquake damage restoration period can be serious. Accordingly, some researchers have attempted to save time and costs incurred from earthquake damage recovery using a repairable PC system (Li *et al.* 2020, Zhang and Li 2021). Li *et al.* (2020) proposed a steel jacketing method to prevent concrete crushing and to replace PC walls. Zhang and Li (2021) devised an energy-dissipating bolt connecting a concrete-filled square steel tube column and RC beam, and they verified its performance through experiments. Although various studies have been conducted, it is hard to find any method for replacing PC beams damaged by earthquake loads. Therefore, a method for rapidly replacing the damaged PC beams was proposed, which can contribute to saving time and costs spent on earthquake damage restoration.

*Corresponding author, Professor
E-mail: kangkim@uos.ac.kr

ISSN: 2092-7614 (Print), 2092-7622 (Online)

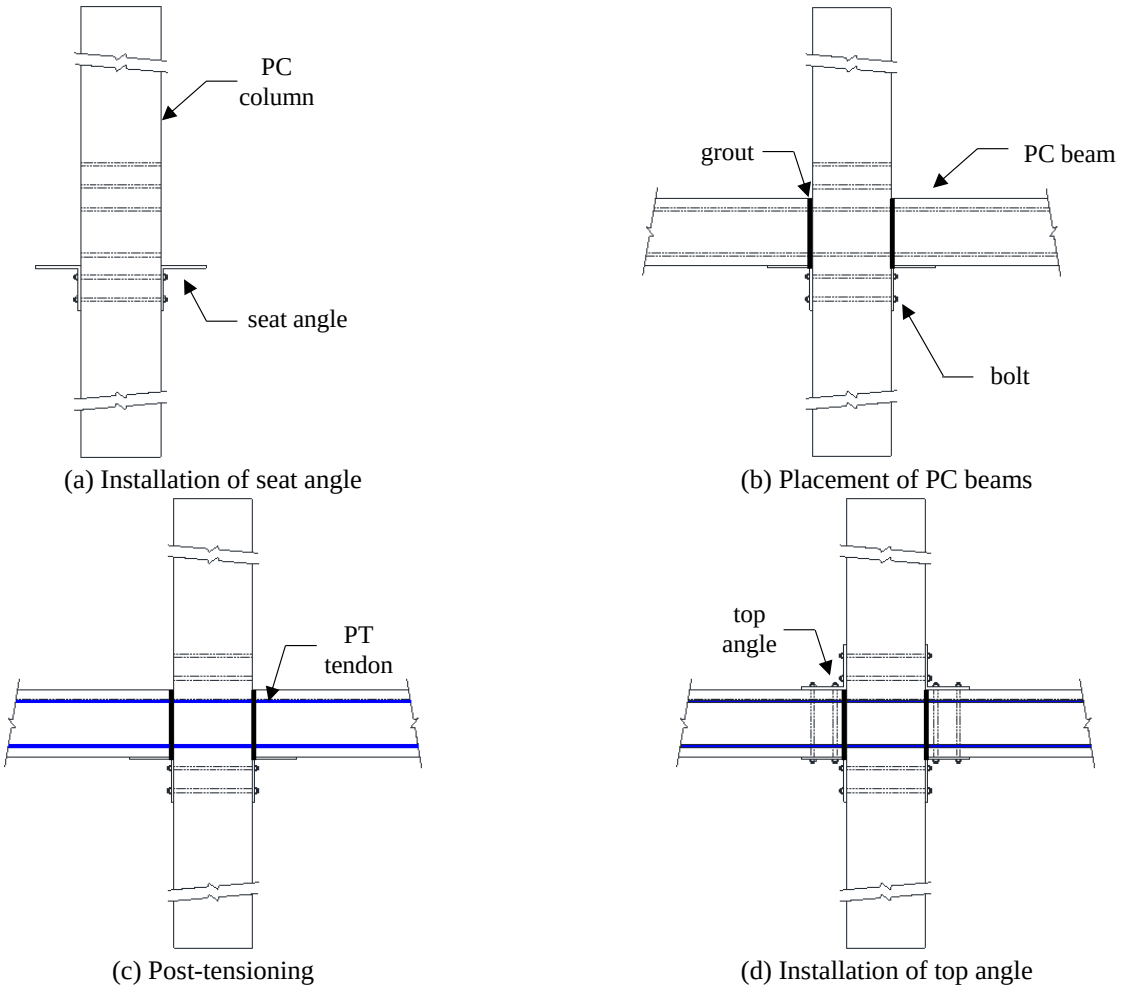

(a) Installation of seat angle (b) Placement of PC beams

(c) Post-tensioning (d) Installation of top angle

Fig. 1 Assembly process of the proposed system

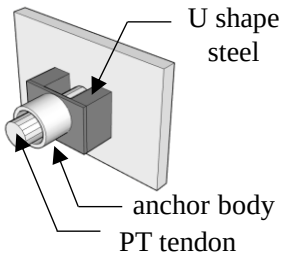

Fig. 2 Details of anchorage at beam ends

2. Experimental program

2.1 Proposed PC connection

In this study, a PC connection system consisting of top-and-seat angle, post-tensioning (PT) tendons, and U-shape steel was developed. The system was devised such that the PT tendon could be cut and the PC beam replaced in the event of damage to the connection caused by an earthquake. Fig. 1 shows the construction process of the developed PC connection system. First, a seat angle is installed at the PC column, and the PC beam is then placed on the seat angle. In other words, the seat angle serves as a corbel on which the PC beam is mounted. When the PC elements are assembled, mortar is poured between the PC column and PC beam at their interface to mitigate problems resulting from construction errors that can occur at the construction site. The tendon is inserted through a sheath embedded in the PC column and PC beam, and PT is introduced. The top angle is subsequently installed to complete the assembly process. Fig. 2 shows the details of the anchorage installed at the end of the beam. A U-shaped steel is installed between the beam end and the anchor head, and the tendon can be cut out through the space in the upper area later, if necessary. If damage occurs because of an earthquake, the tendon is cut, and the top-and-seat angle bolt can be loosened to dismantle the PC beam.

In this study, the seismic performance of the developed PC beam-column connection was evaluated experimentally. A load was applied to the PC beam-column connection specimen at a maximum drift ratio of 2.3%. Then, the PC beam was removed from the connection, and a new PC beam was installed by connecting it to the existing PC column. The repaired PC specimen was loaded, and its structural performances, such as load-displacement relationship, crack patterns, energy dissipation, equivalent viscous damping ratio, strain of steel angle, tendon stress, residual deformation, and joint shear distortion angle, were compared with those of the original PC specimen.

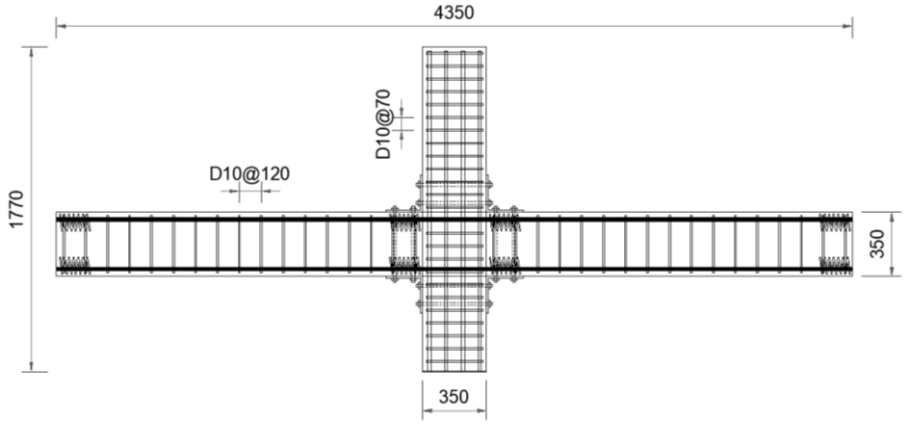

(a) PC beam- PC column connection

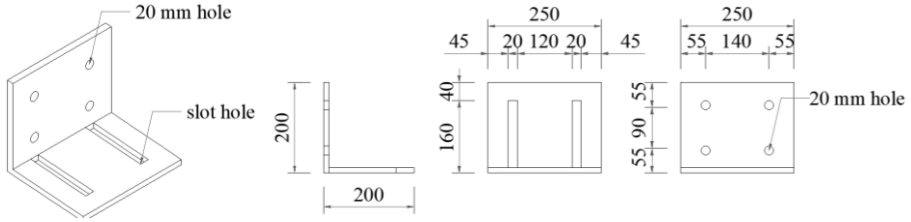

(b) Details of steel angle

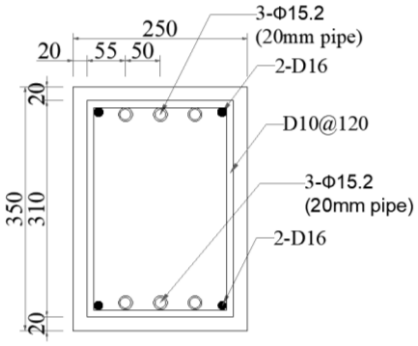

(c) Cross-section of PC beam

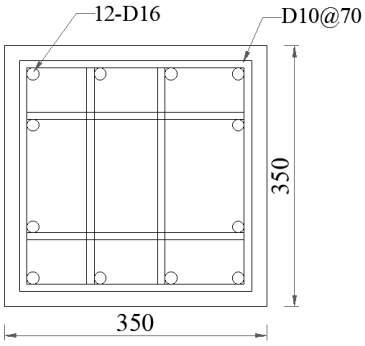

(d) Cross-section of PC column

Fig. 3 Details of test specimens (unit: mm)

2.2 Test specimen

In this study, a five-story office building was set as a prototype structure, and the structural elements were designed based on ACI 318-19 (2019). The span of the prototype structure was 8000 mm, and the floor height was 3500 mm. The cross section of the column was 700×700 mm, while the cross section of the beam was 500×700 mm. For design of the prototype structure, the dead load and live loads were assumed to be 8.4 and 4.0 kN/m^2, respectively. A response modification factor (R-factor) of 8.0 was applied as suggested in ACI 318-19. The specimen dimensions were scaled down by a factor of one-half to accommodate the capability of the testing laboratory. Fig. 3 shows the details of the test specimen. The cross sections of the column and beam were 350×350 and 250×350 mm, respectively. The total span was 4350 mm, and the height was 1770 mm. In the column, 12 D16 reinforcing bars were placed in the longitudinal direction, and D10 closed stirrups were arranged at 70 mm intervals. Furthermore, two D16 reinforcing bars were placed at the top and bottom of the beam. However, because these reinforcing bars did not penetrate the column, they were excluded when calculating the flexural strength of the beam end. Three 15.2 mm diameter (A_{ps}=140 mm^2) mono tendons with a tensile strength of 1860 MPa were placed in both the upper and lower sections of the beam. The total area of the tendon was 420 mm^2. The effective prestress (f_{se}) introduced on the tendon was 40% of the tensile strength (f_{pu}). The D10 closed stirrups were arranged at 120 mm intervals in the longitudinal direction of the beam. In addition, to control the bursting stress of concrete PT, D10 spiral bars were placed at both ends of the beam. The width of the top-and-seat angle was 250 mm, which was equal to the width of the beam. The length and thickness were 200 and 12 mm, respectively. The column and beam members and steel angle were connected with four bolts. However, when the beam was connected to the steel angle, a 160 mm slot hole was made in consideration of constructability.

Fig. 4 shows the process of specimen fabrication. The PC beam and PC column elements were individually manufactured. As mentioned earlier, the members were

- Rebar Assembly - Column formwork - Beam formwork - Concrete pouring

(a) Fabrication of individual PC members

- L shape steel installation - PC member assembly - Tendons inserting - Post-tensioning

(b) Assembly of PC members

- PC beam removal - L shape steel installation - PC member assembly - Post-tensioning

(c) Replacing process of PC beams

Fig. 4 Manufacturing process of test specimens

Table 1 Concrete mix design

Water (kg/m^3)	Cement (kg/m^3)	Coarse aggregate (kg/m^3)	Fine aggregate (kg/m^3)	water cement ratio, W/C (%)
173.5	696.1	854.1	606.4	24.9

assembled in the following order: seat angle installation, PC beam installation, mortar placement between the PC beam and PC column, PT, and top angle installation. After completion of the experiment on the original PC specimen, the tendon was cut using an oxygen cutter through the gap in the upper part of the U-shaped steel. The tendon and top-and-seat angle were removed, and the PC beam was separated from the connection. Then, a new PC beam and top-and-seat angles were installed by connecting it to the column of the original PC specimen. The new PC beam was cast together as the original PC beam, and all details were the same as those of the original PC beam. Table 1 shows the concrete mix design for the PC members, and their compressive strength at the time of the experiment was 35.7 MPa. The compressive strength of the mortar between the PC column and the PC beam was 50 MPa. The yield strength and ultimate strength of the D16 reinforcing bar were 467 and 606 MPa, respectively, and SS275 was used for the steel angle. The flexural strengths calculated by the material test results were 162.4 and 116.6 kN·m in the PC

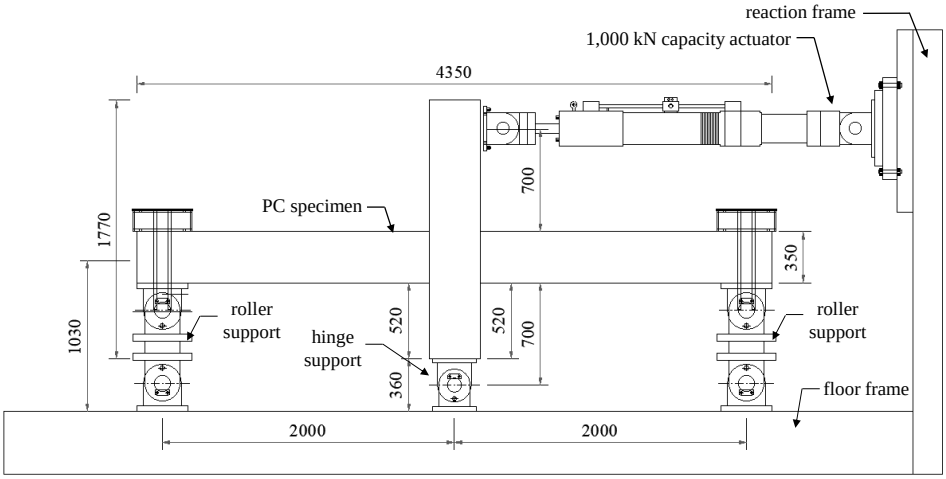

Fig. 5 Test setup (unit: mm)

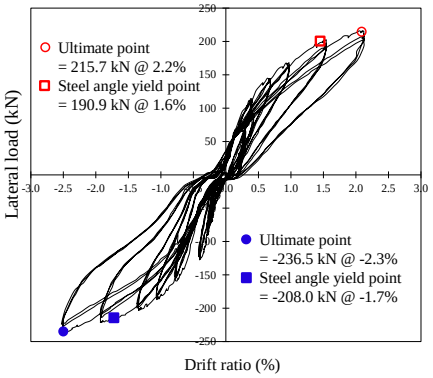

(a) Original PC specimen

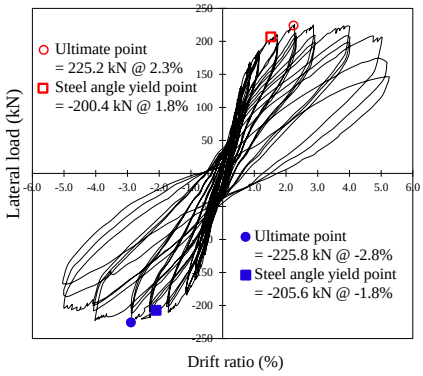

(b) Repaired PC specimen

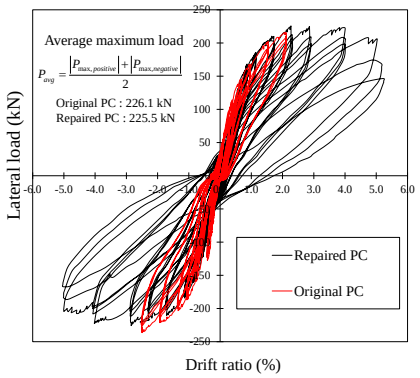

(c) Comparison of test specimens

Fig. 6 Lateral load-drift ratio relationship

column and at the end of the PC beam, respectively. To satisfy the strong-column-weak-beam theory, the structural code suggests that the flexural strength of the column should be 1.2 times greater than that of the beam. The strength ratio of the PC column and PC beam fabricated in this study was 1.39.

2.3 Experimental setup and loading

Fig. 5 shows the experimental setup. In this setting, a 1000 kN capacity actuator connected to the upper part of the PC beam was used to exert the load. The distance from the upper surface of the beam to the loading point was 700 mm. A hinge support was installed at the bottom of the column, while roller supports were placed at both ends of the beam. Based on the load history criteria specified in ACI 374 report (2005), the specimen was subjected to cycling loading three times in the positive direction and three times in the negative direction at drift ratios of 0.2%, 0.25%, 0.35%, 0.5%, 0.75%, 1.0%, 1.5%, 2.0%, 2.5%, 3.5%, and 4.5%. However, in the original PC specimen, the test was terminated at a drift ratio of 2.3%, in which state significant cracks occurred in the beam. The gravity loads were excluded from this test setup.

3. Experimental results

3.1 Hysteretic behavior and crack patterns

Fig. 6 shows the lateral-load-drift-ratio relationship of each specimen, and Fig. 7 shows the crack patterns. When the target drift ratio at each stage was reached, cracks occurred in the positive and negative directions, and they are indicated in red and blue, respectively.

In the original PC specimen, horizontal hairline cracks occurred in the joint at the beginning of the loading, and shear cracks were observed at a drift ratio of 0.75%. The cracks of the PC beam grew significantly at a drift ratio of 1.0%. The maximum crack width in the joint was 0.25 mm at the maximum load. The steel angle yielded at a positive

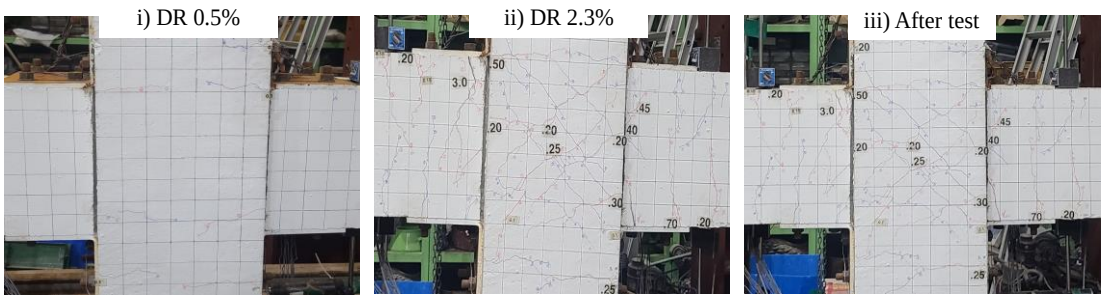

(a) Original PC specimen

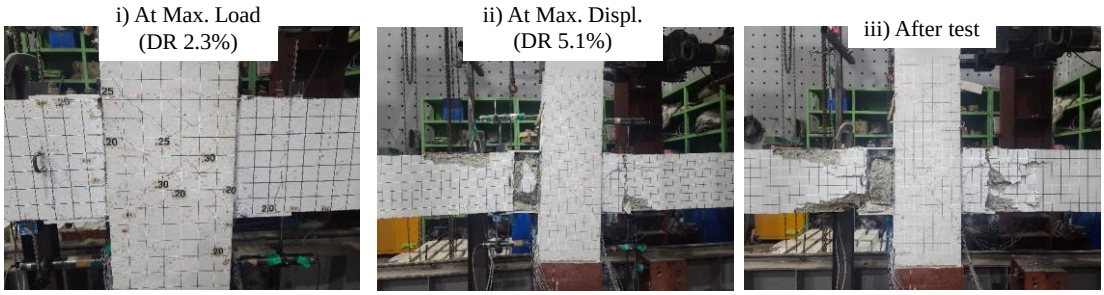

(b) Repaired PC specimen

Fig. 7 Crack patterns

drift ratio of 1.6% and a negative drift ratio of -1.7%. The test was terminated when the cracks near the PC beam-column interface grew significantly in the third cycle at a drift ratio of 2.3%. The original PC specimen exhibited a maximum load of 215.7 kN at a drift ratio of 2.2% in the positive direction and a maximum load of -236.5 kN at a drift ratio of -2.3% in the negative direction.

In the repaired PC specimen, cracks existed in the column panel zone before loading because the new PC beam was connected to the PC column of the original PC specimen. However, additional cracks rarely occurred in the column panel zone at a drift ratio of 2.3% in the repaired PC specimen. The steel angle yielded at a positive drift ratio of 1.8% and a negative drift ratio of -1.8%. The loadings of the original and repaired PC specimens at the yield point of the steel angle were also similar. Even after a drift ratio of 2.3%, which was the maximum loading point of the original PC specimen, additional damage did not occur in the joint of the repaired PC specimen. Cracks continued to grow as damage occurred near the PC beam-column interface (beam end). The maximum loads were 225.2 kN at a drift ratio of 2.3% in the positive direction and -225.8 kN at a drift ratio of -2.8% in the negative direction. The test was terminated when the load decreased to less than 70% of the maximum load in the third cycle at a drift ratio of 5.1%. Fig. 6(c) shows a comparison of the lateral-load-drift-ratio relationship between the original and repaired PC specimens. Overall, the two showed similar behaviors, including initial stiffness, at a drift ratio of 2.3%. The average value of the maximum load in the positive and negative directions of the repaired PC specimen was 225.5 kN, a difference of only 0.2% from that of the original PC specimen. In other words, the initial stiffness and maximum load characteristics of the original PC system were retained even after the PC beam was replaced using the proposed method.

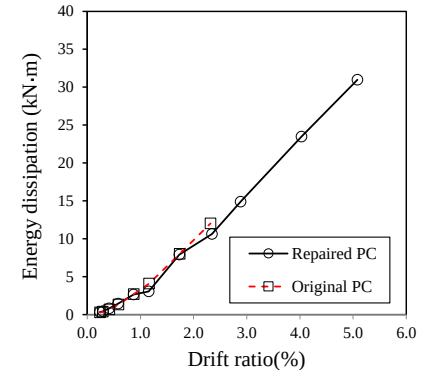

(a) Energy dissipation at each loading cycle

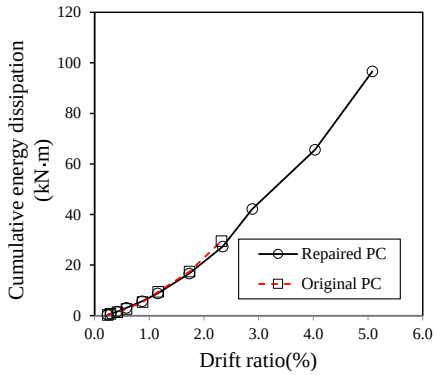

(b) Cumulative energy dissipation

Fig. 8 Comparison of energy dissipation capacities

3.2 Energy dissipation and equivalent viscous damping ratio

Cumulative energy dissipation is an important indicator used to determine the seismic performance of a structure (Ozden *et al.* 2011, Choi *et al.* 2018). Frappa and Pauletta (2022) proposed to install an external steel frame with

dissipative braces. Miani *et al.* (2020) introduced an energy dissipation device to a building with an irregular shape and verified the improvement in structural responses against seismic action. Figs. 8(a) and (b) present the energy dissipation and cumulative energy dissipation of the specimens at each loading cycle. At a drift ratio of 2.3%, the energy dissipation and cumulative energy dissipation of the repaired PC specimen were similar with those of the original PC specimen.

Fig. 9 shows the equivalent viscous damping ratios (ξ_{eq}) (Lim *et al.* 2018) of the two specimens with respect to the drift ratio. The equivalent viscous damping ratio was calculated using Eq. (1).

$$\xi_{eq} = \frac{2A_{loop}}{\pi A_{rect}} \quad (1)$$

Here, A_{rect} is the area of the circumscribed rectangle of the hysteresis loop, and A_{loop} is the energy dissipation of the first cycle. The average value of three cycles at each drift ratio was used. The equivalent viscous damping ratio of a typical RC structure is 5% (Choi *et al.* 2022b). The equivalent viscous damping ratios exceeded 5% in the entire drift ratio range in the original and repaired PC specimens.

3.3 Strain of steel angle

The connection applied with the PT method to connect PC beams and PC columns (Hwang *et al.* 2021, Kim *et al.* 2021, Kim *et al.* 2022, Kim *et al.* 2023) can exhibit relatively low energy dissipation compared with the RC system because of its self-centering behavior. In the proposed method, the top-and-seat angle is used as a corbel that supports the PC beam and simultaneously serves as a damper for energy dissipation. Fig. 10 shows the normalized strain of the steel angle with respect to the increase in drift ratio. The normalized strain was calculated using values measured with a strain gauge attached to the beam area at the seat angle. It was calculated by dividing the strains measured at each drift ratio by the yield strain. It can be determined that the steel angle has yielded when the normalized strain is 1.0. In the positive and negative directions, the strains of the steel angle for the repaired PC specimen were similar to those for the original PC specimen at a drift ratio of 2.3%. Fractures of angles and bolts were not observed until the end of the test. In overall, the steel angle not only exhibited resistance to the load but also had sufficient performance as a vertical support for the PC beam. In this study, however, due to budget limitations, the tests were conducted by fixing the thickness and size of the steel angle and the drilling location for the bolt hole. These parameters including stiffener strengthening of the steel angle can make huge effects on the test results. Therefore, further experimental research would be required to understand such effects in detail.

3.4 Tendon stress

ACI 318-19 (2019) allows stress in the unbonded tendons at nominal flexural strength ($f_{ps,ACI}$) to be calculated in a simplified manner.

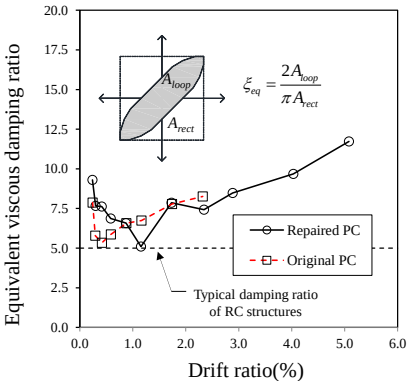

Fig. 9 Comparison of equivalent viscous damping ratios

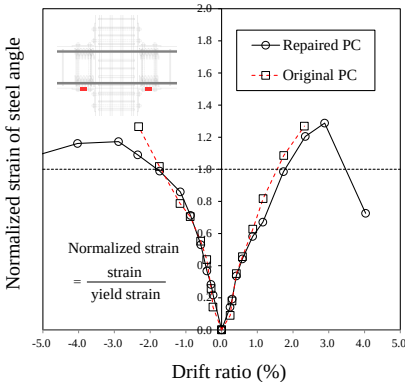

Fig. 10 Strain of steel angle

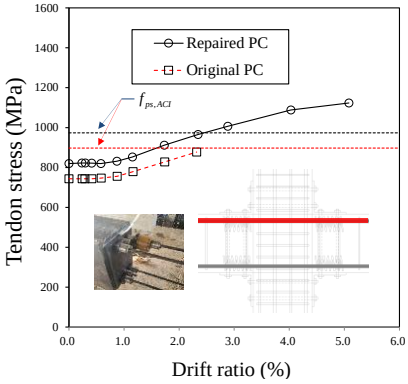

Fig. 11 Tendon stress

$$f_{ps,ACI} = f_{se} + 70 + \frac{f_{ck}}{100\rho_p} \quad (2)$$

Here, f_{ck} is the compressive strength of concrete, ρ_p is the prestressing steel ratio, and f_{se} is the effective stress in the tendon. Fig. 11 shows the change in tendon stress with respect to the increase in the drift ratio, and $f_{ps,ACI}$ (presented in ACI 318-19 (2019)) is also shown in the graph. The effective stresses in the tendon (f_{se}) introduced in the two specimens are slightly different due to limitations of hydraulic jack control. Also, the amount of prestress loss was different in the two specimens. The $f_{ps,ACI}$ of the original PC specimen is represented by the red dotted line, while the black dotted line represents that of the repaired PC specimen. The tendon stress of the original PC specimen immediately before loading was 743 MPa, and the tendon

stress increased after cracks occurred in the joint. As the damage to the joint and PC beam increased, the tendon stress also increased and showed a value similar to that of $f_{ps,ACI}$ at a drift ratio of 2.3%. Immediately before loading, the tendon stress of the repaired PC specimen was 820 MPa. The tendon stress change for the repaired PC specimen was almost the same as that for the original PC specimen at the drift ratio of 2.3%. In addition, the tendon stress of the repaired PC specimen was similar in value to $f_{ps,ACI}$ at the drift ratio of 2.3%.

3.5 Residual deformation

Fig. 12 shows the residual deformation with respect to loading step. Here, the residual deformation is the drift ratio at the point in time when the load becomes zero in the behavior curve of each cycle. The original PC specimen showed residual deformation not exceeding 0.15% up to a drift ratio of 2.3%. The residual deformation of the repaired PC specimen was 0.25% at the drift ratio of 2.3%, and the residual deformation increased gradually as the damage to the PC beam-column interface increased. At the end of the test, the residual deformation was 0.72% at a drift ratio of 5.1%. ACI 374.2R-13 (2013) prescribes that the residual deformation should be less than 1.0% for an applied drift ratio of 2.0% to ensure a life safety performance level. In the repaired PC specimen, the residual deformation did not exceed 1.0%, even at a drift ratio of 5.1%, thus satisfying life safety performance specified in ACI 374.2R-13 (2013).

3.6 Joint shear distortion

Fig. 13 shows the relationship between lateral load and joint shear distortion angle. The joint shear distortion angle (γ_{avg}) (Oesterle *et al.* 1976) was calculated from data measured using two wire gauges in the joint, as follows.

$$\gamma_{avg} = \frac{(d_1'-d_1)d_1-(d_2'-d_2)d_2}{2hL} \quad (3)$$

The repaired PC specimen exhibited a greater joint shear distortion angle compared to the original PC specimen under the identical load. However, the difference was insignificant. This is because cracks were already present in the joint of the repaired PC specimen at the time of the experiment.

3.7 Ductility

As shown in Fig. 14, in this study, the ductility (μ_Δ) of the repaired PC specimen was calculated using the energy balance method (Choi *et al.* 2022a) as follows.

$$\mu_\Delta = \frac{\Delta_u}{\Delta_y} \quad (4)$$

where, Δ_y and Δ_u are the yield and ultimate displacements, respectively. The positive and negative yield displacements of the repaired PC specimen were 20.1 and 20.5 mm, respectively, and the ultimate displacements were 76.5 and 76.0 mm, respectively. The displacement ductility values (μ_Δ) were similar in the positive and negative directions, which were 3.81 and 3.70, respectively.

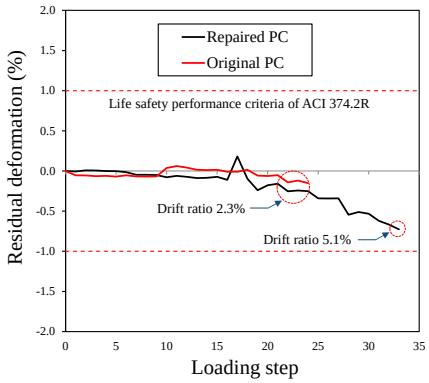

Fig. 12 Comparison of residual deformation

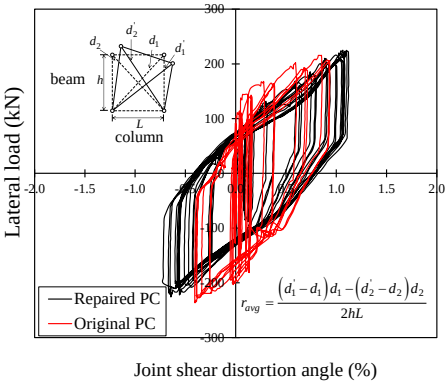

Fig. 13 Comparison of residual deformation

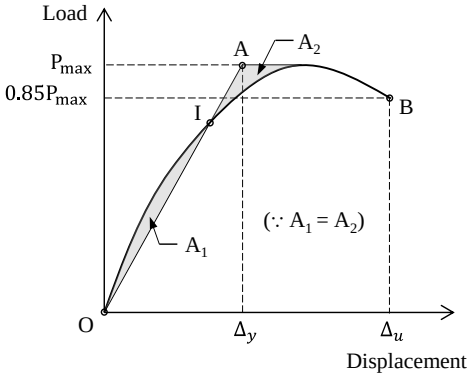

Fig. 14 Displacement ductility (Choi *et al.* 2022a)

4. Conclusions

A system capable of restoring the seismic performance of a PC joint damaged by an earthquake was developed. The system consists of top-and-seat angle, PT tendons, and U-shaped steel and is designed so that the PT tendon can be cut and the PC beam be replaced in the event of damage to the beam elements. The PC connection specimen with the proposed method was loaded to a drift ratio of 2.3%, which caused significant damage to the PC beam. Then, the damaged PC beam was replaced by a new PC beam. The repaired PC connection was subsequently tested, and its seismic performance was compared with that of the original PC specimen. The following conclusions can be drawn from the results.

- No additional damage occurred in the joint of the

repaired PC specimen until a drift ratio of 2.3%, which is the maximum loading point of the original PC specimen, was reached. Even after that, damage occurred mainly at the end of the PC beam near the PC beam-column interface. Overall, the two specimens showed similar structural behaviors up to the drift ratio of 2.3%, including the initial stiffness and maximum load.

• The drift ratios, cumulative energy dissipations, and equivalent viscous damping ratios of the original and repaired PC specimens were similar at a drift ratio of 2.3%. The yield points of the steel angles were also similar to each other. The steel angle not only served as vertical support for the PC beams but also delivered excellent energy dissipation capacity under lateral loads.

• The changes in tendon stress of the two specimens were similar. At a drift ratio of approximately 2.3%, the tendon stress values of both specimens reached the stress value for unbonded tendons at the nominal flexural strength suggested by ACI 318-19. It is concluded that, when significant damage occurs to the PC beam at a drift ratio of approximately 2.3%, the proposed system can be used to replace the damaged beam element to facilitate structural restoration.

• In the repaired PC specimen, the residual deformation did not exceed 1.0%, even at a drift ratio of 5.1%, which was the termination point of the test, thus ensuring the life safety performance level specified in ACI 374.2R.

Acknowledgments

This research was supported by the Basic Science Research Program through the National Research Foundation of Korea (NRF) funded by the Ministry of Education (2021R1I1A1A01040337).

References

ACI Committee 318 (2019), Building Code Requirements for Structural Concrete (ACI 318-19) and Commentary (ACI 318R-19), American Concrete Institute, Farmington Hills, MI, USA.

ACI Committee 374 (2005), Acceptance Criteria for Moment Frames Based on Structural Testing and Commentary (ACI 374.1-05), American Concrete Institute, Farmington Hills, MI, USA.

ACI Committee 374 (2013), Guide for Testing Reinforced Concrete Structural Elements under Slowly Applied Simulated Seismic Loads (ACI 374.2R-13), American Concrete Institute, Farmington Hills, MI, USA.

Barbhuiya, S. and Choudhury, A. M. (2015), "A study on the size effect of RC beam-column connections under cyclic loading", *Eng. Struct.* **95**, 1-7. https://doi.org/10.1016/j.engstruct.2015.03.052.

Choi, S.H., Kim, J.H., Jeong, H. and Kim, K.S. (2022a), "Seismic behavior of beam-column joints with different concrete compressive strengths", *J. Build. Eng.*, **52**, 104484. https://doi.org/10.1016/j.jobe.2022.104484.

Choi, S.H., Heo, I., Darkhanbat, K., Choi, S.M. and Kim, K.S. (2022b), "Experimental and numerical study on pre-cambered deep deck-plate system", *Comput. Concrete*, **30**(6), 445-453. https://doi.org/10.12989/cac.2022.30.6.445.

Choi, S.H., Hwang, J.H., Han, S.J., Joo, H.E., Kim, J.H. and Kim, K.S. (2021), "Experimental study of punching shear in post-tensioned slabs with unbonded tendons", *Struct. Eng. Mech.*, **79**(4), 507-516. https://doi.org/10.12989/sem.2021.79.4.507.

Choi, S.H., Hwang, J.H., Lee, D.H., Kim, K.S., Zhang, D. and Kim, J.R. (2018), "Experimental study on RC frame structures strengthened by externally-anchored PC wall panels", *Comput. Concrete*, **22**(4), 383-393. https://doi.org/10.12989/cac.2018.22.4.383.

Choi, S.H., Heo, I., Kim, J.H., Jeong, H., Lee, J.Y. and Kim, K.S. (2022c), "Flexural behavior of post-tensioned precast concrete girder at negative moment region," *Comput. Concrete*, **30**(1), 75-83. https://doi.org/10.12989/cac.2022.30.1.075.

Frappa, G. and Pauletta, M. (2022), "Seismic retrofitting of a reinforced concrete building with strongly different stiffness in the main directions", *Proceedings of 14th fib International PhD Symposium in Civil Engineering*, Rome, Italy, September.

Han, S.J., Kim, J.H., Choi, S.H., Heo, I. and Kim, K.S. (2022), "Web-shear strength of steel-concrete composite beams with prestressed wide flange and hollowed steel webs: Experimental and practical approach", *Struct. Eng. Mech.*, **84**(3), 311-321. https://doi.org/10.12989/sem.2022.84.3.311.

Hwang, J.H., Choi, S.H., Lee, D.H., Kim, K.S. and Kwon, O.S. (2021), "Seismic behaviour of post-tensioned precast concrete beam-column connections", *Mag. Concrete Res.*, **73**(9), 433-447. https://doi.org/10.1680/jmacr.19.00083.

Jin, K., Kitayama, K., Song, S. and Kanemoto, K. (2016), "Shear capacity of precast prestressed concrete beam-column joint assembled by unbonded tendon", *ACI Struct. J.*, **114**(6), 51-61. https://doi.org/10.14359/51689148.

Karimi Pour, A. (2022), "Experimental and numerical evaluation of steel fibres RC patterns influence on the seismic behaviour of the exterior concrete beam-column connections", *Eng. Struct.*, **263**, 114358. https://doi.org/10.1016/j.engstruct.2022.114358.

Kim, J.H., Choi, S.H., Han. S.J., Hwang, J.H., Jeong, H. and Kim, K.S. (2023), "Effect of beam elongation phenomenon on lateral load resistance of RC frame", *J. Build. Eng.*, **65**, 105764. https://doi.org/10.1016/j.jobe.2022.105764.

Kim, J.H., Choi, S.H., Hwang, J.H., Jeong, H., Han, S.J. and Kim, K.S. (2021), "Experimental study on lateral behavior of post-tensioned precast beam-column joints", *Struct.*, **33**, 841-854. https://doi.org/10.1016/j.istruc.2021.04.095.

Kim, J.H., Lee, D., Choi, S.H., Jeong, H. and Kim, K.S. (2022), "Seismic performance of precast multi-span frame system integrated by unbonded tendons", *ACI Struct. J.*, **119**(5), 193-206. https://doi.org/10.14359/51734801.

Li, B., Kulkarni, S.A. and Leong, C.L. (2009), "Seismic performance of precast hybrid-steel concrete connections", *J. Earthq. Eng.*, **13**(5), 667-689. https://doi.org/10.1080/13632460902837793.

Li, X., Wu, G., Kurama, Y.C. and Cui, H. (2020), "Experimental comparisons of repairable precast concrete shear walls with a monolithic cast-in-place wall", *Eng. Struct.*, **216**, 110671. https://doi.org/10.1016/j.engstruct.2020.110671.

Lim, W.Y., Kang, T.H.K. and Hong, S.G. (2018), "Effect of reinforcement details on seismic behavior of precast concrete wall-steel coupling beam systems", *ACI Struct. J.*, **115**(6), 1751-1763. https://doi.org/10.14359/51702414.

Lu, C., Dong, B.Q., Pan, J.L., Shan, Q.F., Hanfi, A. and Yin, W. (2018) "An investigation on the behavior of a new connection for precast structures under reverse cyclic loading", *Eng. Struct.*, **169**, 131-140. https://doi.org/10.1016/j.engstruct.2018.05.041.

Miani, M., Di Marco, C., Frappa, G. and Pauletta, M. (2020), "Effects of dissipative systems on the seismic behavior of irregular buildings—Two case studies", *Build.*, **10**, 202. https://doi.org/10.3390/buildings10110202.

Oesterle, R.G., Fiorato, A.E., Johal, L.S., Carpenter, J.E., Russell,

H.G. and Corley, W.G. (1976), "*Earthquake resistant structural walls - Tests of isolated walls*", PB271-467; Construction Technology Laboratories, Portland Cement Association.

Ozden, S., Akguzel, U. and Ozturan, T. (2011), "Seismic strengthening of infilled reinforced concrete frames with composite matrials", *ACI Struct.*, **108**(4), 414-422. https://doi.org/10.14359/51682981.

Paulay, T., Park, R. and Priestley, M.J.N. (1978), "Reinforced concrete beam-column joints under seismic actions", *ACI Struct. J.*, **75**(11), 585-593. https://doi.org/10.14359/10971.

Pauletta. M., Marco, C.D., Frappa, G., Miani, M., Campione, G. and Russo, G. (2021), "Seismic behavior of exterior RC beam-column joints without code-specified ties in the joint core", *Eng. Struct.*, **228**, 111542. https://doi.org/10.1016/j.engstruct.2020.111542.

Parastesh, H., Hajirasouliha, I. and Ramezani, R. (2014), "A new ductile moment-resisting connection for precast concrete frames in seismic regions: An experimental investigation", *Eng. Struct.*, **270**, 144-157. https://doi.org/10.1016/j.engstruct.2014.04.001.

Peloso, S., Casarotti, C., Dacarro, F. and Sinopoli, G. (2020), "Response of an existing two-storey RC frame designed for gravity loads: In situ pushover tests and numerical analyses", *Build.*, **10**(12), 227. https://doi.org/10.3390/buildings10120227.

Tazarv, M., Boudaqa, A. and Tuhin, I. (2020), "Repairable precast moment-resisting buildings: Part I—Experimental investigations", *ACI Struct. J.*, **117**(6), 147-170. https://doi.org/10.14359/51728061.

Yu, Z., Lv, X., Ding, F. and Peng, X. (2019), "Seismic performance of precast concrete columns with improved U-type reinforcement ferrule connections", *Int. J. Concrete Struct. Mater.*, **13**, 1-18. https://doi.org/10.1186/s40069-019-0368-6.

Zhang, X. and Li, B. (2020), "Seismic performance of RC beam-column joints constructed with engineered cementitious composites", *J. Struct. Eng.*, **146**(12), 04020271. https://doi.org/10.1061/(ASCE)ST.1943-541X.0002824.

Zhang, Y. and Li, D. (2021), "Seismic behavior and design of repairable precast RC beam-concrete-filled square steel tube column joints with energy-dissipating bolts", *J. Build. Eng.*, **44**, 103419. https://doi.org/10.1016/j.jobe.2021.103419.

CC